Resonant Acoustic Propagation and Negative Density in Liquid Foams

Juliette Pierre, Benjamin Dollet, Valentin Leroy

Resonant Acoustic Propagation and Negative Density in Liquid Foams

Juliette Pierre,[1] Benjamin Dollet,[2] and Valentin Leroy[1]

[1] *Laboratoire Matière et Systèmes Complexes, Université Paris-Diderot, CNRS (UMR 7057), Paris, France*
[2] *Institut de Physique de Rennes, Université Rennes 1, CNRS (UMR 6251), Rennes, France*

(Dated: October 17, 2013)

We measured the dispersion relation for acoustic longitudinal waves in liquid foams, over a broad frequency range (60–600 kHz). Strong dispersion was found, with two non-dispersive behaviors, separated by a negative density regime. A new model, based on the coupled displacements of films, Plateau borders and gas in the foam, rationalizes all the experimental findings.

Liquid foams, dispersions of gas bubbles in a liquid matrix stabilized by surfactants [1], are present in a wide range of industrial applications, from food and personal care to ore flotation and enhanced oil recovery [2]. They are opaque materials, hence difficult to characterize in depth, and new ways of probing them are highly desirable. Acoustic probes are good candidates, since they are unexpensive and nonintrusive, and widely used as such in nondestructive testing [3]. However, surprisingly little is known about liquid foam acoustics, contrary to other multiphasic media such as porous media [4], colloidal suspensions, or emulsions [5, 6]. Most of the few existing experimental studies reported speeds of sound of order 50 m/s [7–9], close to the so-called Wood model [10]. The latter treats foams as an effective medium, which density and compressibility are averages of those of the gas and liquid phases, weighted by their respective volume fractions. However, much higher speeds of sound, of order 200 m/s, were also measured [11, 12], and some studies reported a resonant behavior [13, 14], reminiscent of the Minnaert resonance of a single bubble in an unbounded liquid [15], which is the key ingredient of acoustic propagation through dilute bubbly liquids [16, 17]. In this Letter, we use a novel setup [18] to measure speed of sound and attenuation through liquid foams over a large range of frequencies f (60–600 kHz) and bubble radii (15–50 μm). Our results are explained by a new model, which fully reconciles all aforementioned different viewpoints on liquid foam acoustics. In particular, we show that liquid foams are natural acoustic metamaterials, exhibiting a negative effective density over a large range of frequencies and bubble sizes.

The general principle of our technique is to measure the complex transmission of short ultrasonic pulses through a foam sample of known thickness. From this complex transmission, we can determine the effective complex wavevector as a function of frequency: $k = \omega/v + \mathrm{i}\alpha$, with $\omega = 2\pi f$, and v and α the phase velocity and attenuation of sound. In an ageing foam, the bubble median radius R increases over time by Ostwald ripening [1]. Hence, making measurements at different times, we obtain $k(\omega, R)$, the complex wavevector as a function of frequency and median radius. Some aspects of the ultrasonic technique and the foam production and characterization are briefly described below; more details can be found in [18] for the former, and [19] for the latter.

Transmission measurements were performed with two broadband air transducers. The thickness of the foam samples was set to 0.5 mm by sandwiching them between two plastic films, which were as thin as possible to allow a good transmission of ultrasound. An inversion procedure was used to deduce the effective wavevector k of sound in the foam from the complex transmission measured through the three-layer system {film-foam-film}. This procedure relied on the assumption that either the effective density ρ_{eff} or the effective compressibility χ_{eff} were known. Guided by the model presented below, we assumed that the effective compressibility of the liquid foam was given by the usual mixture law: $\chi_{\mathrm{eff}} = \Phi\chi_\ell + (1-\Phi)\chi_g$, where Φ is the liquid volume fraction and $\chi_{\ell,g}$ the compressibility of the liquid and gaseous phase.

Liquid foams with liquid volume fractions ranging from 3% to 22% were obtained by the two-syringe method [19]. The foaming liquid was an aqueous solution containing 10 g/L of sodium dodecyl sulfate to ensure good foamability, and 0.5 g/L of xanthane to reduce drainage. Given the small thickness of the samples (0.5 mm), the typical radius of the bubbles (less than 50 μm) and the presence of xanthane, we were able to neglect the gradient of liquid fraction due to gravity [20]. The gaseous phase was air saturated with vapor of C_6F_{14}, an insoluble gas that slows down Ostwald ripening. Thus, the typical time over which the foam was changing ($\sim$ 10 minutes) was long enough not only to consider the acoustic measurements as instantaneous, but also to perform bubble size measurements [19]. To do that, we took a small subsample of the foam from the syringe, and pour it on a liquid bath to obtain a bubble raft, a two-dimensional structure easy to image. Assuming that the left-over in the syringe was ageing the same way as the foam between the films, we were able to follow the time evolution of the bubble size distribution. We found lognormal distributions $\exp\{-[\ln(r/R)]^2/2\epsilon^2\}/(r\epsilon\sqrt{2\pi})$ with a median radius R going from 15 to 50 μm in 90 minutes, and a polydispersity of $\epsilon \simeq 0.4$ without significant time evolution (Fig. 1c).

Measurements shown in Fig. 1a clearly indicate that

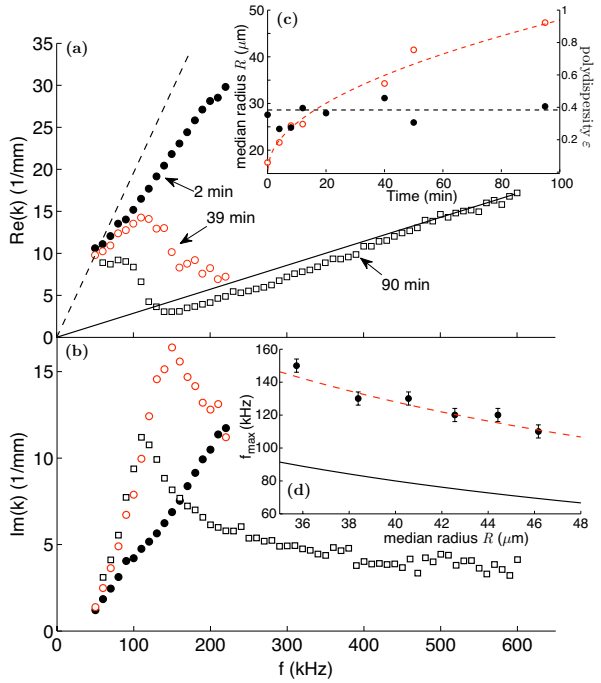

FIG. 1: (a) Real part of the wavenumber as a function of the frequency, measured at three di erent ageing times in a liquid foam with = 11%. Lines show dispersion curves for constant velocities of 32 m/s (dash) and 220 m/s (solid). (b) Imaginary part of the wavenumber. (c) Median radius of the bubbles (○) and polydispersity (●) as functions of the ageing time. (d) Frequency of the maximum of attenuation as a function of the median radius; solid line is the Minnaert frequency f_M, dashed line is $1.6 f_M$.

the propagation of acoustic waves in a liquid foam is dispersive. The phase velocity at low frequencies is close to the value predicted by Wood law: $v = [(\Phi\rho_\ell + (1-\Phi)\rho_g)(\Phi\chi_\ell + (1-\Phi)\chi_g)]^{-1/2} = 32\,\mathrm{m/s}$ for $\Phi = 11\%$. But it significantly deviates from this value as the frequency increases and the foam ages. At $t = 90$ min the phase velocity is of the order of 220 m/s.

The attenuation (Fig. 1b) is also frequency-dependent and evolves as the foam ages. For the longest times (i.e. largest bubbles), a peak is clearly visible. One can report the frequency of the maximum of attenuation $f_{\max}$ as a function of R (Fig. 1d), and compare it with the Minnaert frequency $f_M = \sqrt{3\gamma P_0/\rho}/(2\pi R)$ [15], where P_0 is the pressure of the gas in the bubbles, and γ the ratio of the specific heat capacities. Taking $f_{\max} = 1.6 f_M$ gives a reasonable law (dashed line in Fig. 1d), suggesting an effective Minnaert resonance, as proposed in previous experiments [13, 14]. However, the Minnaert frequency is calculated for a single bubble in an infinite volume of liquid of density ρ, and for highly concentrated media such as foams, it seems unrealistic. Replacing ρ by the actual density of the surrounding medium $\Phi\rho$ would lead to $3 f_M$ for $\Phi = 11\%$, larger than the 1.6 factor we measured. Moreover, it predicts a resonance frequency that decreases with Φ, contrary to our experiments (Fig. 2). Finally, the range of radii over which we measured a maximum of attenuation (Fig. 1d) is too small to validate a scaling law in $f_{\max} \sim 1/R$. Instead of limiting our analysis to the peak of attenuation, we can take advantage of all the radii by collapsing the data on a master curve: we plot kR^p as a function of fR^p, with an exponent p. As shown in Fig 3, a good collapse is obtained for $p = 1.5$, as suggested by the model we present below. This indicates that R is the key parameter that governs the frequency dependence of the acoustic behavior of the foam (the polydispersity being almost constant with time).

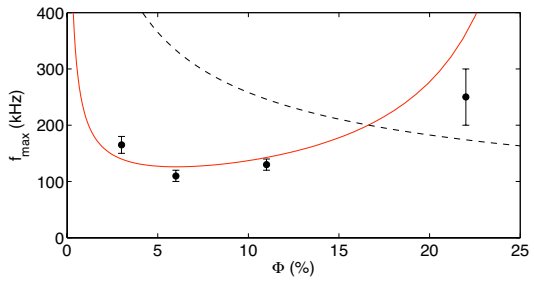

FIG. 2: Frequency of the maximum of attenuation as a function of the liquid fraction, for median radii of 40 μm. Dashed line is the Minnaert resonance frequency with an e ective density: $\omega_M/\sqrt{\ }$. Solid line is the prediction of our model.

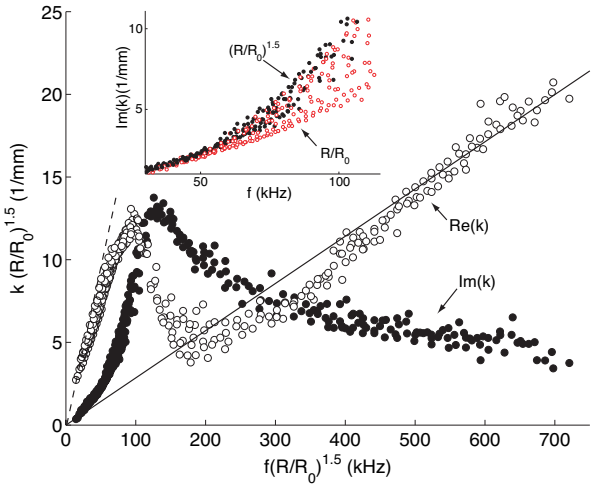

FIG. 3: Rescaled dispersion relation for a reference median radius of $R_0 = 40\,\mu$m. Lines are for constant velocities of 32 (dash) and 220 m/s (solid). Inset: the $R^{-1.5}$ scaling (solid symbols) is better than the R^{-1} one (open symbols).

Contrary to usual bubbly media, bubbles in a foam are in contact through thin films, separated by Plateau borders and vertices [1]. Usually films contain a very small amount of water, hence films and Plateau borders have very different inertia, whose influence we shall now

model. In first approximation, we neglect polydispersity, and we idealize the foam as a one-dimensional array of spatial periodicity d of the following unit cell (Fig. 4a): a flexible, circular film of thickness e and radius a, attached to a rigid Plateau border of mass m_p, forming a ring of external radius b, and surrounded by air of density ρ_a.

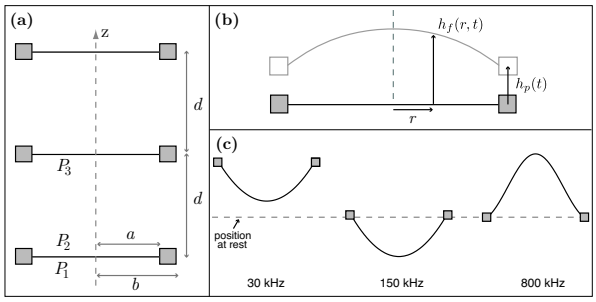

FIG. 4: (a) Sketch of the idealized foam structure: a periodic array of films and Plateau borders, separated by a distance d. (b) Zoom on one unit cell: the flexible film is attached to a rigid Plateau border sketched as a square. (c) Profiles of a $20\,\mu$m radius film at three di erent frequencies, as predicted by the model.

To predict the acoustic wavevector, we need to model the behavior of the unit cell under compression (effective compressibility $\chi_{\rm eff}$), as well as its average displacement (effective density $\rho_{\rm eff}$): $k^2 = \omega^2 \rho_{\rm eff}\chi_{\rm eff}$. Our model geometry is similar to that of Lee *et al.* [21], who studied sound propagation through an array of elastic membranes; in particular, it can be shown exactly as in [21] that the effective compressibility is given by the mixture law.

The effective density, on the other hand, is more complicated. As sound propagates, the films vibrate in response to pressure variations, and entrain the Plateau borders. On a given unit cell, a pressure difference $\Delta P = P_2 - P_1$ across the film tends to curve it, owing to the surface tension σ. With $h_f(r,t) = \mathrm{Re}[z_f(r)\mathrm{e}^{-\mathrm{i}\omega t}]$, we get $z_f(r) = AJ_0(qr) + \Delta P/(2\sigma q)$, where $q = \omega\sqrt{\rho e/2\sigma}$ is the wavenumber of capillary waves on the film [27], and J_0 the Bessel function of order 0 of the first kind [22].

The unknown constant A is determined by matching the film motion with that of the Plateau border, which is driven by the pressure difference ΔP and by the traction of the film $-4\pi\sigma a(\partial h_f/\partial r)_{r=a}$. Furthermore, it is well known in foam rheology that the relative motion of a film and a Plateau border involves a significant dissipation in the transition region [23], but it has not been yet investigated in the kHz range. Hence, we simply assume that there is a force on the Plateau border opposite to its motion relative to the film in contact, of the form: $-2\pi a\xi(\partial^2 h_f/\partial t\partial r)_{r=a}$. With $h_p(t) = \mathrm{Re}(z_p\mathrm{e}^{-\mathrm{i}\omega t})$, we finally get the full profile

$$z_f(r) = \frac{\Delta P}{\rho e\omega^2}\left[1 - \frac{m_p - m_f(b^2-a^2)/a^2}{m_p + m_f(1-\mathrm{i}\delta)\mathcal{H}(qa)}\frac{J_0(qr)}{J_0(qa)}\right], \quad (1)$$

where $m_f = \pi a^2 e\rho$ is the mass of the film, $\delta = \omega\xi/2\sigma$ a viscous damping constant, and $\mathcal{H}(qa) = 2J_1(qa)/[qaJ_0(qa)]$.

We now consider the motion of air between two consecutive films, which is driven by the pressure difference $P_2 - P_3$. As the acoustic wavelength λ is much larger than the typical bubble size (in air $\lambda = 485\,\mu$m at 700 kHz), we may consider that the whole air of the unit cell moves as one block with displacement z_a given by $-m_a\omega^2 z_a = (P_2 - P_3)\pi b^2$, where m_a is the mass of the air in the cell. Moreover, the air in contact with the film and Plateau border is also entrained by their motion. By continuity of displacement, we simply assume that z_a equals the average displacement of the film and Plateau border: $z_a = (1-x)z_p + \frac{2x}{a^2}\int_0^a r z_f(r)\mathrm{d}r$, where $x = a^2/b^2$ is the fraction of the surface covered by the film, whose empirical dependence on Φ has been established by Princen [24]: $x = 1 - 3.20[7.70 + (1-\Phi)/\Phi]^{-1/2}$. Hence we find that the average displacement z_a of the unit cell is $\omega^2\rho_{\rm eff}z_a = (P_3 - P_1)/d$, with an effective density $\rho_{\rm eff} = (1-\Phi)\rho_a + \Phi'\rho$, where the frequency-dependent effective liquid volume fraction Φ' is given by

$$\Phi' = \frac{\Phi_p + \Phi_f(1-\mathrm{i}\delta)\mathcal{H}(qa)}{1 + \left(x^2\frac{\Phi_f+\Phi_p}{\Phi_f} - 2x\right)[1-\mathcal{H}(qa)] - \mathrm{i}\delta x\mathcal{H}(qa)}, \quad (2)$$

with Φ_p and Φ_f the volume fraction of liquid respectively in the Plateau border and in the film: $\Phi_p + \Phi_f = \Phi$. Eq. (2) predicts two asymptotic non-dispersive behaviors. At low frequencies, $\mathcal{H}(qa) \simeq 1$, hence $\mathrm{Re}\,\Phi' = \Phi$: the Wood approximation is recovered. At high frequencies, $\mathcal{H}(qa)$ tends towards 0, leading to $\mathrm{Re}\,(1/\Phi') = (1-x)^2/\Phi_p + x^2/\Phi_f$. If $\Phi_f \ll \Phi_p[x/(1-x)]^2$ (i.e. films contain a negligible part of water, but with a non-negligible surface) this last formula reduces to x^2/Φ_f, similar to Kann's model [12], which considers sound propagation as that in air, modified only by the inertia of the films.

The transition between the two asymptotic regimes can be inspected by noting that $1 - \mathcal{H}(qa) \sim_0 -(qa)^2/8$. Thus, within the approximation $\Phi_p \gg \Phi_f|1 - 2/x|$, Eq. (2) becomes $\Phi' \simeq \Phi_p/[1 - (\omega/\omega_0)^2 - \mathrm{i}x\delta]$, similar to the response function of an harmonic oscillator with a resonance frequency $\omega_0^2 = 16\sigma\Phi_f/(\rho a^2 e x^2\Phi)$ and a damping factor $x\delta$. Interestingly, this resonance frequency depends neither on a nor on e since $\Phi_f = n_f\pi a^2 e$, n_f being the number per unit volume of films perpendicular to the direction of propagation. If we consider that there are N such films per bubble, we obtain $n_f = 3N\Phi/[4\pi R^3\exp(9\epsilon^2/2)]$ and the resonance frequency becomes

$$\omega_0^2 = \frac{12N\sigma(1-\Phi)}{x^2\rho\Phi R^3\exp(9\epsilon^2/2)}, \quad (3)$$

which predicts the experimentally observed $R^{-1.5}$ scaling law. The mechanism of this resonance is different

from Minnaert's one: inertia also comes from water, but here the restoring force is due to the tension of the film, not the compressibility of air. Eq. (3) captures well the dependence on Φ of the frequency of the maximum of attenuation, as shown in Fig. 2. For an increasing liquid fraction, the increase of density ($1/\sqrt{\Phi}$ term, as in the modified-Minnaert relation) is balanced by the shrinkage of the films ($1/x$ term).

To go beyond and get a quantitative prediction over the full range of frequencies and sizes, we refine the model and include polydispersity, as explained in SM1. Briefly, this amounts to changing $\mathcal{H}(qa)$ by $\mathcal{I} = \int \mathcal{H}(qa)a^2 n(a)\mathrm{d}a / \int a^2 n(a)\mathrm{d}a$ in the expression (2) of the effective liquid fraction, with $n(a)$ the distribution of film radii. If we assume that this distribution is log-normal with a median radius a_0, a polydispersity ϵ_f and a total number of films per unit volume n_f, the model counts a total of nine parameters. Three are known: $\sigma = 35\,\mathrm{mN/m}$, $\Phi_p = 11\%$, $\epsilon = 0.4$. Four can be estimated: $x(\Phi = 11\%) = 0.2$, $n_f = 1620\,\mathrm{films\ per\ mm^3}$ (assuming $N = 1$), $a_0 = 15\,\mu\mathrm{m}$ (taking an average of 6 films per bubble imposes $x = 1.5(a_0/R)^2$) and $\epsilon_f = 0.4$ (same polydispersity as for bubble radii). The two remaining parameters were fitted to the experimental data: ξ governs the width of the resonance, e the high-frequency effective density. With $\xi = 7.4 \times 10^{-7}\,\mathrm{kg/s}$ and $e = 70\,\mathrm{nm}$, the model agrees well with the experimental data (Fig. 5). This value of e is compatible with the usual measurements of film thickness, of a few tens of nm [1]. It is less easy to compare ξ to any standard measurement, and the study of the microscopic dissipation mechanisms at high frequency is left as a perspective of our work.

A salient feature of our study is the existence of a negative real part of the density over an extended range of frequencies (100 to 350 kHz). The mechanism of this negative effective density is well illustrated by looking at the displacement of a film and a Plateau border predicted by (1) (see Fig. 4c). At low frequencies, both the film and the Plateau border move in phase with the incoming pressure. At high frequencies, only the film moves. At intermediate frequencies, while the Plateau border has a small in-phase displacement, the film moves out of phase with an amplitude large enough to compensate for its small inertia. The net average movement of the system is then out of phase, which leads to a negative effective density [28].

As a conclusion, we have evidenced two regimes for the sound propagation in a liquid foam, separated by a resonance. Our study reconciles the seemingly contradictory results previously reported: a low speed of sound, compatible with Wood's model, at low frequency and small bubble size; a much higher one, slightly lower than that in air, at high frequency and large bubble size; and a resonance in between, with a maximum of attenuation. This rich variety of behaviors is fully captured by a model coupling the motion of air, films and Plateau borders.

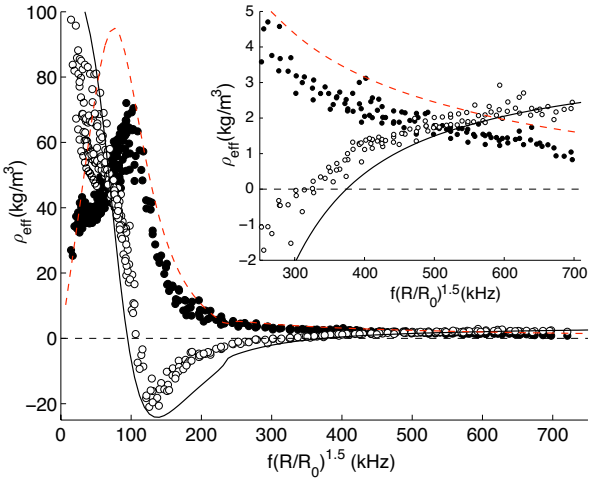

FIG. 5: Comparison between the measured e ective complex density (○ real part, • imaginary part) and prediction of the equivalent of Eq. (2) in the polydisperse model (see SM1).

This makes acoustic probing of foams promising, since each of these regimes is sensitive to different parameters. The low frequency regime gives access to the liquid fraction. The resonance is linked to surface tension. The high frequency regime depends on the film thickness, which is interesting in practice since no existing technique enables to measure it in a bulk of foam.

Finally, we have shown for the first time that liquid foams are naturally acoustic metamaterials, with an effective negative density over an extended range of frequency and bubble size (e.g. 100 to 350 kHz for $R = 40\ \mu\mathrm{m}$). Moreover, in contrast with most existing metamaterials [25, 26], which are synthetic, highly ordered materials, this property exists even though the foam is isotropic and polydisperse. Our findings could thus bring fresh insight to design metamaterials for applications such as acoustic insulation.

We acknowledge funding support from the Agence Nationale de la Recherche (project SAMOUSSE, ANR-11-BS09-001). We thank J.-C. Bacri, C. Gay, F. Graner and A. Saint-Jalmes for fruitful discussions.

[1] I. Cantat, S. Cohen-Addad, F. Elias, F. Graner, R. Höhler, O. Pitois, F. Rouyer, A. Saint-Jalmes, *Foams*, edited by S. J. Cox, Oxford University Press (2013).
[2] *Foam Engineering: Fundamentals and Applications*, edited by P. Stevenson, Wiley (2012).
[3] J. Blitz, G. Simpson, *Ultrasonic Methods of Non-destructive Testing*, Chapman & Hall (1996).
[4] K. Attenborough, *Physics Reports* **82**, 179 (1982).
[5] A. S. Dukhin, P. J. Goetz, *Adv. Colloid Interface Sci.* **92**, 72 (2001).
[6] R. E. Challis, M. J. W. Powey, M. L. Mather, A. K.

Holmes, *Rep. Prog. Phys.* **68**, 1541 (2005).
[7] I. I. Goldfarb, I. R. Shreiber, F. I. Vafina, *J. Acoust. Soc. Am.* **92**, 2756 (1992).
[8] I. Goldfarb, Z. Orenbach, I. Schreiber, F. Vafina, *Shock Waves* **7**, 77 (1997).
[9] N. Mujica, S. Fauve, *Phys. Rev. E* **66**, 021404 (2002).
[10] A. B. Wood, *A Textbook of Sound*, Bell (1944).
[11] N. T. Moxon, A. C. Torrance, S. B. Richardson, *Appl. Acoust.* **24**, 193 (1988).
[12] K. B. Kann, *Colloids Surf. A* **263**, 315 (2005).
[13] J. Ding, F.W. Tsaur, A. Lips, A. Akay, *Phys. Rev. E* **75**, 041601 (2007).
[14] I. Ben Salem, R. M. Guillermic, C. Sample, V. Leroy, A. Saint-Jalmes, B. Dollet, *Soft Matter*, **9**, 1194 (2013).
[15] M. Minnaert, *Phil. Mag.* **16**, 235 (1933).
[16] K. W. Commander, A. Prosperetti, *J. Acoust. Soc. Am.* **85**, 732 (1989).
[17] V. Leroy, A. Strybulevych, J. H. Page, M. Scanlon, *J. Acoust. Soc. Am.* **123**, 1931 (2008).
[18] J. Pierre, F. Elias, V. Leroy, *Ultrasonics* **53**, 622 (2013).
[19] J. Pierre, R. M. Guillermic, F. Elias, W. Drenckhan, V. Leroy, *Eur. Phys. J. E* **36**, 113 (2013).
[20] A. Maestro, W. Drenckhan, E. Rio, and R. Höhler, *Soft Matter*, **9**, 2531 (2013).
[21] S. H. Lee, C. M. Park, Y. M. Seo, Z. G. Wang, C. K. Kim, *Phys. Lett. A* **373**, 4464 (2009).
[22] see for instance chapter 4 in L. E. Kinsler, A. R. Frey, A. B. Coppens, J. V. Sanders, *Fundamental of Acoustics*, John Wiley & Sons (2000).
[23] I. Cantat, *Phys. Fluids* **25**, 031303 (2013).
[24] H. M. Princen, *J. Colloid Interface Sci.* **105**, 150 (1985).
[25] N. Fang, D. Xi, J. Xu, M. Ambati, W. Srituravanich, C. Sun, X. Zhang, *Nature Materials* **5**, 452 (2006).
[26] M. Yang, G. Ma, Z. Yang, P. Sheng, *Phys. Rev. Lett.* **110**, 134301 (2013).
[27] This is an approximate formula for q, see discussion in SM1 and J. G. H. Joosten, *J. Chem. Phys.* **80**, 2363 (1984), Y. Couder, J. M. Chomaz, M. Rabaud, *Physica D* **37**, 384 (1989), P. Sens, C. Marques, J. F. Joanny, *Langmuir* **9**, 3212 (1993)
[28] A movie showing the oscillations of the film and BP is available in SM2.

Resonant Acoustic Propagation and Negative Density in Liquid Foams
Supplemental material

Juliette Pierre,[1] Benjamin Dollet,[2] and Valentin Leroy[1]

[1] *Laboratoire Matière et Systèmes Complexes, Université Paris-Diderot, CNRS (UMR 7057), Paris, France*
[2] *Institut de Physique de Rennes, Université Rennes 1, CNRS (UMR 6251), Rennes, France*

(Dated: October 17, 2013)

DISPERSION RELATION OF CAPILLARY WAVES ON A SOAP FILM

The dispersion relation $q^2 = \rho e\omega^2/2\sigma$ of capillary waves on a soap film neglects both air inertia, and dissipative effects. This is questionable, and air inertia is indeed known to have a significant effect on the vibrations of soap films [1]. Accounting for it usually requires to solve the full velocity field in air, coupled *locally* with the film motion through the continuity of normal stress at the air/liquid interface. Our approach is simpler: we model this coupling not locally, but *globally*, by imposing the continuity of displacement between air and the system {film–Plateau border} as a global constraint.

Dissipation is also essential in our model. Without it, q is real, the function $a \mapsto \mathcal{H}(qa)$ diverges as soon as qa is a zero of J_0, and our model does not capture the high-frequency regime. Any source of dissipation adds an imaginary part on q, which suppresses these divergences and smoothes out the behavior of $\mathcal{H}(qa)$.

Among possible sources of dissipation, the role of liquid viscosity has been previously investigated [2, 3]. It modifies the dispersion relation, which becomes $\bar{\omega}^2+2\mathrm{i}\zeta\bar{\omega}-1 = 0$, with a rescaled frequency $\bar{\omega} = \omega\sqrt{\rho e/(2\sigma q^2)}$, and a dimensionless viscous damping $\zeta = \frac{1}{6}\nu q^3\sqrt{\rho e^5/2\sigma}$. With $\nu = 10^{-6}$ m^2/s the kinematic viscosity of our solution, and taking from the data $e = 70$ nm, and $q = 2\pi/a_0$ with $a_0 = 15$ μm, we compute $\zeta = 2\times10^{-6} \ll 1$, hence $q \simeq (1+\mathrm{i}\zeta)\omega\sqrt{\rho e/2\sigma}$. This imaginary correction is much too small to fit the experimental data (see Fig. 1); in particular, it does not regularize enough the behavior of the effective density at high frequency. Hence we neglected liquid viscosity, and investigated viscous dissipation in the air put into motion close to the film.

Briefly, this is done by solving Navier–Stokes equation in the air and the potential flow for the liquid within the film, which are coupled by the following boundary conditions: continuity of normal and tangential stress, and continuity of normal velocity, at the interface. The calculations give:

$$0 = \left(\frac{1}{2}qe - \mathrm{i}\frac{\nu_a q^3 e}{\omega}\right)(\bar{\omega}^2-1) + \frac{\rho_a}{\rho}\bar{\omega}^2.$$

Treating the effect of air as a perturbation, we deduce from this dispersion relation that $q = (1+\mathrm{i}\zeta_a)\omega\sqrt{\rho e/2\sigma}$ with $\zeta_a = \eta_a/\sqrt{\rho e\sigma/2}$. With $\eta_a = 1.8\times10^{-5}$ Pa s the dynamic viscosity of air, we compute $\zeta_a = 0.02$, which is four orders of magnitude larger than ζ: viscous dissipation in the liquid is negligible compared to that in air in our range of experimental parameters. Including this correction is necessary to give a satisfactory agreement between the data and the model at high frequency, since it enables $\mathcal{H}(qa)$ to tend smoothly towards 0 (see Fig. 1). However, it is still insufficient to fit the data over the full range of frequency and size. In particular, it predicts a much too peaked resonance, and an increase of the real part of the effective density, which is not seen in experiments (Fig. 5 in the Letter). This is why we plugged an extra dissipation in the model, at the transition region between the film and the Plateau border.

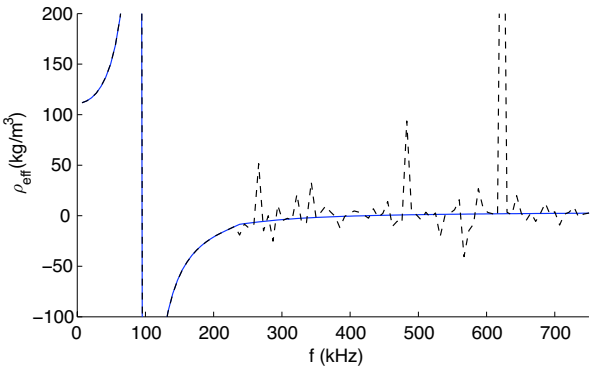

FIG. 1: Prediction of the model for the real part of the effective density as a function of frequency for two sources of dissipation: viscous losses in the liquid (dashed line), and viscous losses in the air (solid line). The dissipation in the meniscus is neglected ($\xi = 0$) and the other parameters are as in Fig. 5 of the Letter.

EXTENSION OF THE MODEL TO THE POLYDISPERSE CASE

The monodisperse model (Eq. (2) of the Letter) does not lead to a good comparison with the experimental data. In particular, the regime of negative effective density cannot be described properly (see Fig. 2). A refined model that takes the polydispersity into account is thus needed.

Let us consider a thin slice of foam oriented perpendicularly to the direction of propagation of the acoustic

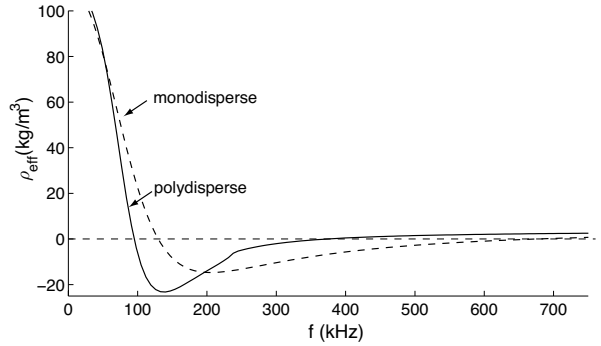

FIG. 2: Comparison of the monodisperse and polydisperse models for the effective density (real part) as a function of frequency for $R = 40$ μm; see the Letter for the value of the other parameters.

wave. We note $n(a)\mathrm{d}a$ the number of films per unit volume whose radius is between a and $a + \mathrm{d}a$ and whose orientation is perpendicular to the direction of propagation. We choose the volume V of the slice in such a way that there is in average one film across its thickness: $V \int \pi a^2 n(a)\mathrm{d}a = xS$, where S is the surface of the considered slice. Each film has a profile given by $z_f(a;r) = A(a)J_0(qr) + \Delta P/(2\sigma q^2)$, *i.e.* as in the monodisperse case but with A that depends on a. The wavenumber q may also depend on a, through the thickness of the film; nevertheless, for simplicity, we consider that all the films have the same thickness e. This approximation is encouraged by the good collapse of the experimental data with a scaling on R only, indicating that film thickness variations with ageing time can be neglected. The $A(a)$ constant is still given by continuity of displacement on the border of each film: $z_f(a;r=a) = z_p$, where z_p it the displacement of all the Plateau borders. We indeed assume that the network of Plateau borders in the slice move as a block, with no deformation. These Plateau borders, of total mass m_p, are driven by the pressure difference ΔP and by the traction of all the films, leading to $-m_p\omega^2 z_p = -(1-x)S\Delta P - 4\pi\sigma(1-\mathrm{i}\delta)V \int an(a)\mathrm{d}a \frac{\partial z_f}{\partial r}(a;r=a)$. Dividing by V, and noting that $\int \pi a^2 n(a)\mathrm{d}a = \Phi_f/e$, we get

$$-\rho\Phi_p\omega^2 z_p = -\frac{(1-x)\Phi_f\Delta P}{xe} + 4\pi\sigma(1-\mathrm{i}\delta)\Sigma, \qquad (1)$$

with $\Sigma = \int an(a)\mathrm{d}aA(a)qJ_1(qa)$. Continuity of displacement gives the second condition on z_p: $z_p = A(a)J_0(qa) + \Delta P/(2\sigma q^2)$, hence:

$$\Sigma = \frac{1}{2\pi}\left(q^2 z_p - \frac{\Delta P}{2\sigma}\right)\int n(a)\mathrm{d}a\pi a^2\mathcal{H}(qa). \qquad (2)$$

Inserting Eq. (2) into Eq. (1), we get

$$z_p = -\frac{\Delta P}{\omega^2\rho e}\frac{(x-1)/x - (1-\mathrm{i}\delta)\mathcal{I}}{\Phi_p/\Phi_f + (1-\mathrm{i}\delta)\mathcal{I}},$$

with $\mathcal{I} = (e/\Phi_f)\int \mathcal{H}(qa)n(a)\pi a^2\mathrm{d}a$. The profile of a film of radius a can then be calculated, from which we deduce the average displacement of a film of radius a:

$$\begin{aligned}\langle z_f(a)\rangle &= \frac{1}{\pi a^2}\int_0^a 2\pi r\mathrm{d}r z_f(a;r) \\ &= \frac{\Delta P}{\omega^2\rho e}\left[1 - \mathcal{H}(qa)\frac{\Phi_p/\Phi_f - (1-x)/x}{\Phi_p/\Phi_f + (1-\mathrm{i}\delta)\mathcal{I}}\right].\end{aligned}$$

Then the average amplitude of displacement of the films and Plateau borders, which we assume identical to the air displacement z_a, can be calculated:

$$\begin{aligned}z_a &= (1-x)z_p + \frac{V}{S}\int n(a)\mathrm{d}a\pi a^2\langle z_f(a)\rangle \\ &= \frac{\Delta P S}{V\omega^2\rho}\frac{1 + \left(x^2\frac{\Phi_f+\Phi_p}{\Phi_f} - 2x\right)(1-\mathcal{I}) - \mathrm{i}\delta x\mathcal{I}}{\Phi_p + \Phi_f(1-\mathrm{i}\delta)\mathcal{I}},\end{aligned}$$

leading at the same effective density as in the monodisperse case with $\mathcal{I}$ instead of $\mathcal{H}$ (see Eq. (2) in the Letter).

Assuming a lognormal distribution for the films radii: $n(a) = \exp\{-[\ln(a/a_0)]^2/2\epsilon_f^2\}/(a\epsilon_f\sqrt{2\pi})$, we can use the relation $\int n(a)a^p\mathrm{d}p = n_f a_0^p \exp(p^2\epsilon_f^2/2)$ where n_f is the number of films per unit volume, a_0 their median radius and ϵ_f their polydispersity. The low-frequency limit of Φ' then becomes

$$\Phi' \simeq \frac{\Phi_p}{1 - (\omega/\omega_0)^2 - \mathrm{i}x\delta}, \qquad (3)$$

with a polydisperse resonance angular frequency given by

$$\omega_0^2 = \frac{12N\sigma(1-\Phi)}{x^2\rho\Phi R^3\exp(9\epsilon^2/2 + 4\epsilon_f^2)}. \qquad (4)$$

Note that, as in the monodisperse case, the radii and thicknesses of the films are not parameters of the resonance. On the other hand, the polydispersity of the films plays a role, and decreases significantly the resonance frequency (Fig. 2). It is therefore necessary to include it to get a good prediction of the resonance, and also of the extent of the range of negative density.

The maximum of attenuation of the acoustic waves in the foam is reached when the real part of the density is minimum and negative, which is given by $\omega_{\max} = \omega_0\sqrt{1+x\delta}$. We used this relation in Fig. 2 of the Letter, in which $\omega_{\max}$ is reported as a function of Φ.

[1] Y. Couder, J. M. Chomaz, M. Rabaud, *Physica D* **37**, 384 (1989).
[2] J. G. H. Joosten, *J. Chem. Phys.* **80**, 2363 (1984).
[3] P. Sens, C. Marques, J. F. Joanny, *Langmuir* **9**, 3212 (1993).